SCIENCE CHINA
Physics, Mechanics & Astronomy

• Article •
Special Topic: Modern Acoustics

doi: 10.1007/s11433-013-5092-7

Delamination damage detection of laminated composite beams using air-coupled ultrasonic transducers

LIU ZengHua*, YU HongTao, HE CunFu & WU Bin

College of Mechanical Engineering and Applied Electronics Technology, Beijing University of Technology, Beijing 100124, China

Received July 3, 2012; accepted August 31, 2012

Air-coupled ultrasonic transducers are used to generate and receive Lamb waves in quasi-isotropic laminated composite beams for delamination detection. The influence of incident angle on the excited mode is studied. Numerical calculation and experimental results show that a pure Lamb wave mode can be generated if the transmitting transducer is oriented at a specific angle, and the receiving transducer can either be oriented to detect the same mode as that generated by the transmitter or to detect another mode generated by mode conversion at a defect. A three-dimensional finite element model is created to predict the interaction of Lamb waves with delamination, and some unique mechanisms of interaction between A_0 mode Lamb waves and delamination are revealed in detail. The experimental results obtained on laminated composite beam using air-coupled ultrasonic transducers are well in accordance with finite element simulation results. Research results show that air-coupled ultrasonic guided waves can be used for delamination damage detection effectively in laminated composite beams.

delamination detection, composite beam, Lamb wave mode, air-coupled ultrasonic transducer, three-dimensional finite element simulation

PACS number(s): 43.20.Mv, 43.35.Zc, 81.70.Cv

Citation: Liu Z H, Yu H T, He C F, et al. Delamination damage detection of laminated composite beams using air-coupled ultrasonic transducers. Sci China-Phys Mech Astron, doi: 10.1007/s11433-013-5092-7

1 Introduction

Composite materials such as carbon fiber/epoxy plastic (CF/EP) laminates have been found substantially increasing applications in fields of aerospace, civil and mechanical engineering over the past decades. Properties such as high strength and stiffness, directional tailorability, low coefficient of thermal expansion, resistance to environmental effects make composite materials the first choice for many applications. However, damage may appear in composite laminates because of impact or fatigue loadings. Delamination is one of the most common types of damage in composite materials [1]. Delamination damage may significantly reduce compressive strength, stiffness, damping properties and results in structural failure. In order to ensure the integrity and reliability of the materials, nondestructive testing & evaluation (NDT & E) must be performed during manufacturing process and maintenance.

Ultrasonic testing methods, especially Lamb wave-based techniques, have received considerable attention over the past decades. Lamb wave-based techniques have a number of attractive advantages: Lamb waves can travel over a long distance even in materials with a high attenuation ratio and various Lamb modes can interrogate the entire thickness of the laminate [2]. To implement delamination damage detection with Lamb waves, it is necessary to understand the mechanism of interaction between Lamb waves and delamination damage. Finite element (FE) anlaysis is the most powerful numerical tool used to analyze this mechanism. Guo and Cawley [3] studied the interaction of S_0 mode

*Corresponding author (email: liuzenghua@bjut.edu.cn)

Lamb waves with delamination in an eight-layer cross-ply composite laminate $[(0/90)_2]_S$ by finite element analysis. Delaminations were introduced at various interfaces between the layers. It was demonstrated that when S_0 mode encounters a delamination along its propagation path, a reflected wave is shown to be generated. However, the amplitude of reflection wave is strongly dependent on the position of the delamination through the thickness of the laminate, and no wave reflection takes place when shear stress is zero at that interface. Ramadas et al. [4] studied the interaction of A_0 mode Lamb waves with symmetric delaminations in a quasi-isotropic laminated composite plate using two-dimensional FE model. It was found that when the A_0 mode interacts with a symmetric delamination, it generates a new mode, S_0, which is confined only to sub-laminates. Peng et al. [5] investigated the interaction of Lamb waves with the delamination in an eight-ply CF/EP laminate by two-dimensional spectral element method. The interactions of both the S_0 mode and A_0 mode with the delamination were investigated. The results show that the A_0 mode is more suitable for the identification of delamination in composite laminate, especially when the delamination is in the symmetric plane.

Conventional ultrasonic testing systems, employing piezoelectric transducers with liquid couplants or immersion transducers with water couplant, can degrade these materials through absorption of these liquid couplants [6]. It is difficult to maintain the consistency of the coupling conditions during the test, especially when the surface of the test piece is not flat [7]. Air-coupled ultrasonic testing emerges as a promising method for non-contact testing. Another advantage of air-coupled inspection is that a relatively pure Lamb wave mode can be excited with appropriate incident angle. Electrostatic, air-coupled ultrasonic transducers were used for the first time in the 1970s for propagating waves in solids [8]. The acoustic impedance is 45.6, 4.65 and 0.00041 for steel-4340, carbon/epoxy composite (60 v/o) and air (20°C) respectively [9]. There is a large difference between the acoustic impedance of metals and air. As a result, little research work was done in ultrasonic testing for metal materials with air-coupled ultrasonic transducers during the past decades. However, when it comes to ultrasonic testing for composite materials, air-coupled ultrasonic transducers are still widely used [10–12]. More recently, the development of high efficiency transducers [13] and improvements in ultrasonic transmitting and receiving instruments (e.g. high dB preamplifier) make air-coupled ultrasonic testing a powerful method. Yan et al. [14] investigated the identification of impact delaminations in a carbon-epoxy composite plate. A pair of air-coupled ultrasonic transducers were used to generate and receive Lamb waves in the composite plate in a through transmission mode. The defects were detected and located quite well through a guided wave imaging method based on the probabilistic damage detection concept. Takahashi et al. [15] developed 2 MHz air-coupled ultrasonic transducers using P(VDF/TrFE) piezoelectric films and obtained high resolution acoustic images with the developed transducers. Raišutis et al. [16] studied the testing of square-shape carbon fiber reinforced plastics rods employing the developed air-coupled technique in a pitch-catch mode for cases of conventional transsion and advanced back-scattering configurations. It was found that the actual sizes of the internal defects have been clearly detected using reception of the back-scattered waves over the edges of the defective regions only. Schmidt et al. [17] studied damage evolution in wound glass fiber reinforced tubes due to impact and subsequent biaxial cyclic loading using air-coupled ultrasonic transducers. Air-coupled guided wave scans for delamination characterization due to impact agree well with visual inspection.

In this study, the most suitable Lamb mode and frequency range are selected first of all through theoretical consideration and numerical calculation. Furthermore, the coincidence incident angle of air-coupled ultrasonic transducer to excite a pure Lamb wave mode is obtained according to theoretical calculation and experimental study. Then three-dimensional (3D) FE models are created by running Matlab scripts to generate input files for ABAQUS. The interaction of A_0 mode Lamb waves with delamination is investigated in detail with the help of the developed FE models. For the experimental study, one air-coupled ultrasonic transducer is oriented to excite pure A_0 mode Lamb waves in a 16-layer CF/EP composite laminate beam, and the other air-coupled ultrasonic transducer is oriented to capture the reflected wave and transmitted wave respectively. A method of locating and sizing the delamination is proposed for quantitative detection of delamination damage in composite beam.

2 Theoretical consideration and numerical calculation

2.1 Appropriate Lamb wave mode selection

When a free plate is excited, the excitation will generate guided Lamb waves in the plate. Lamb waves are composed of the coupling between longitudinal and shear modes. Lamb waves contain various wave modes. All Lamb wave modes are dispersive (i.e. their velocity is dependent on frequency) [18].Transfer matrix method and global matrix method are often used to obtain the dispersion curves in laminates [19]. For the tested 16-layer quasi-isotropic CF/EP composite laminate $[(0/45/90/-45)2]_S$ in this study, each layer has a thickness of 0.14 mm. The material properties are listed in Table 1. Phase velocity dispersion curves of Lamb waves along 0° direction are plotted in Figure 1. As seen in Figure 1, the number of co-existing wave modes goes up as the frequency increases. High order Lamb wave

modes begin to appear when the frequency increases to 0.35 MHz. Since the existence of many Lamb wave modes makes the analysis difficult, an appropriate frequency range must be chosen to isolate fundamental symmetric mode (S_0) and anti-symmetric mode (A_0). In this research, the excitation frequency must be below 0.35 MHz to isolate the fundamental modes. The attenuation coefficients of ultrasonic waves in air and composite materials increase as the excitation frequency increases. However, as shown in Figure 1, Lamb wave modes are more disperse in the low frequency range. Here, 0.2 MHz is chosen as the appropriate excitation center frequency to reach a good balance between attenuation and dispersion. Mode shapes of S_0 and A_0 modes at 0.2 MHz, as shown in Figure 2, reveal that S_0 mode has mainly in-plane surface displacement whereas A_0 mode has mainly out-of-plane surface displacement. Thus, A_0 mode can be easily collected with air-coupled ultrasonic transducer in contrast to S_0 mode. The wavelength of A_0 mode is shorter than that of S_0 mode at the same frequency. Besides, A_0 mode can interrogate the entire thickness of the laminate but S_0 mode cannot detect delamination in the symmetric plane [3]. A_0 mode is the best choice, in recognition of the principle in ultrasonic testing that the wavelength of the selected mode must be lower than or equal to the size of the damage.

2.2 Incident angle determination of air-coupled ultrasonic transducer for Lamb wave excitation

When ultrasonic waves travel through air and hit an interface between air and plate at an angle, both reflected and refracted waves are produced. Refracted waves go on traveling within the plate. After multiple reflections and accompanying mode conversion, one or more Lamb wave modes are excited. The phase velocity of excited Lamb wave mode is directly linked to incident angle by the Snell's law, formulated by [20]

$$\theta_m = \sin^{-1}\left(\frac{c_c}{c_m}\right), \tag{1}$$

where c_c is the phase velocity of the wave propagating in the couplant (air in this research), c_m is the phase velocity of the Lamb wave mode m, and θ_m defines the orientation of the transducers required to excite and collect mode m. As the velocity of air and the phase velocity of Lamb waves (shown in Figure 1) are known, incident angle disperse curves of Lamb waves along 0° direction can be obtained by solving eq. (1). The results are shown in Figure 3, corresponding to wave propagates in 0° direction. These curves help in optimizing the orientation of the transmitting and receiving air-coupled ultrasonic transducers. A certain Lamb wave mode will be excited if the angular and frequency excitation zones coincide with one certain curve in Figure 3. The theoretical coincidence angle for pure A_0 mode generation at 0.2 MHz for this research is 14°, and this will be verified experimentally in the subsequent section.

2.3 Convergence condition of 3D FE model

This research is based on the assumptions of linear elasticity. The FE models are created to compute the response of the specimens to a certain excitation. In this way, the wave

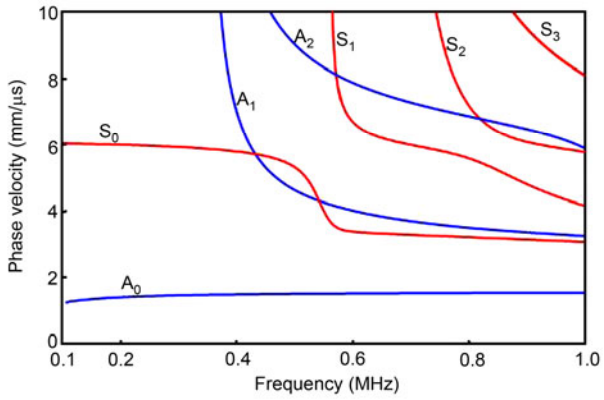

Figure 1 (Color online) Phase velocity dispersion curves of Lamb waves along 0° direction for the tested 16-layer CF/EP laminate.

Table 1 Material properties of a 16-layer CF/EP laminate

E_1 (GPa)	E_2 (GPa)	E_3 (GPa)	G_{12} (GPa)	G_{13} (GPa)	G_{23} (GPa)	ν_{12}	ν_{13}	ν_{23}	ρ (kg/m^3)
135	8.8	8.8	4.47	4.47	3.45	0.3	0.3	0.34	1560

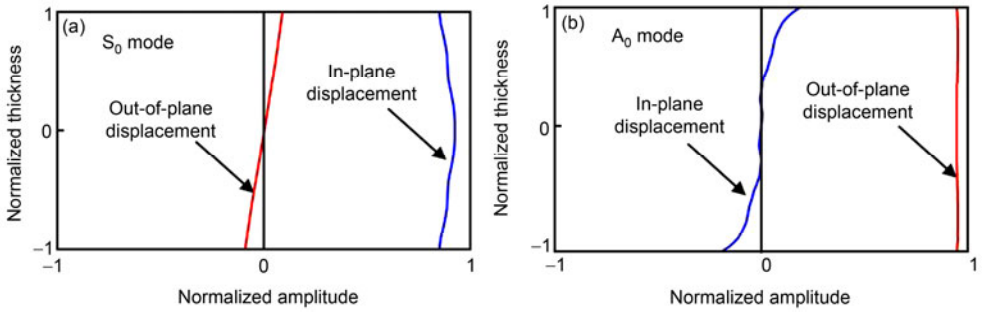

Figure 2 (Color online) Mode shapes of fundamental Lamb wave modes: (a) S_0 mode, (b) A_0 mode.

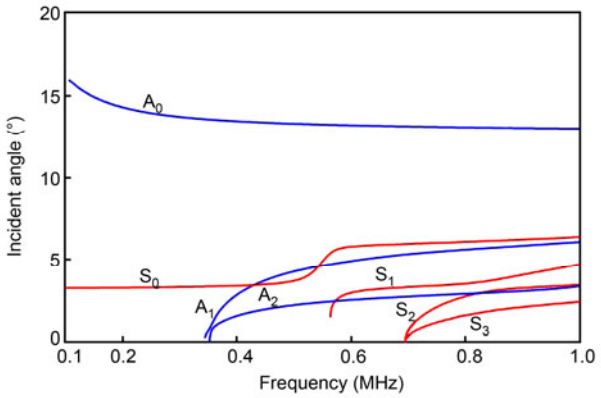

Figure 3 (Color online) Incident angle dispersion curves of Lamb waves along 0° direction for the tested 16-layer CF/EP laminate.

propagation and interaction with delamination damage can be simulated. One finite element method [21] was used to calculate the displacements of every point of the spatial mesh that defines the specimen, as a function of time. The basic equation of equilibrium governing the linear dynamic response of the system is formulated [22,23]

$$MU + C\dot{U} + K\ddot{U} = R(t), \tag{2}$$

where M, C and K are the mass, damping, and stiffness matrices, $\boldsymbol{R}(t)$ is the external load vector, and U, $\dot{U}$, and $\ddot{U}$ are the displacement, velocity, and acceleration of the nodes comprising the FE mesh. Spatial and temporal resolutions of the FE models are critical for the convergence of these numerical results. The size of the elements must be chosen in a manner [24] so that the propagating waves are spatially resolved, formulated by

$$l_{\mathrm{e}} \leqslant \frac{\lambda_{\min}}{10}, \tag{3}$$

where l_{e} is the element length and $\lambda_{\min}$ is the shortest wavelength of interest. It is recommended that more than 10 nodes per wavelength should be used when meshing. The integration time step (incremental time step in ABAQUS), Δt, is the step size for which eq. (2) is solved. It is ruled by [21]

$$\Delta t \leqslant \frac{l_{\mathrm{e}}}{c_{\max}}, \tag{4}$$

where l_{e} is the element length and $c_{\max}$ is the velocity of the fastest wave of interest in the specimen.

2.4 Experimental determination of phase and group velocities of Lamb waves

The phase velocity is the velocity at which wave of an individual frequency travels. The phase velocity c_{P} of Lamb waves is given in terms of the wavelength λ, the period T and the frequency f as:

$$c_{\mathrm{P}} = \frac{\lambda}{T} = \lambda f. \tag{5}$$

The wavelength can also be expressed in terms of wavenumber k and phase period 2π as:

$$\lambda = \frac{2\pi}{k}, \tag{6}$$

where wavenumber k is commonly expressed as the number of wavelengths per 2π units of distance, and its physical significance is the varying rate of phase with the propagation distance. According to its physical significance, wavenumber k can also be expressed as:

$$k = \frac{\Delta\varphi}{\Delta x}, \tag{7}$$

where $\Delta\varphi$ is the phase change between two signals s_1 and s_2 corresponding to adjacent positions x_1 and x_2, and Δx is the distance between adjacent positions x_1 and x_2 as well as wave propagation distance. Here, Δx should be below one wavelength, so as the phase varies in one phase period. Substituting the wavelength λ from eq. (6) and the wavenumber k from eq. (7) into eq. (5) generates a new phase velocity equation as:

$$c_{\mathrm{P}} = \frac{2\pi f}{k} = \frac{2\pi f \Delta x}{\Delta\varphi}. \tag{8}$$

The phase velocity can be experimentally measured by placing two receiving transducers at positions x_1 and x_2 with a distance Δx and extracting phase change from received signals. The phase change can be calculated by applying Fourier transform (FT) to the received signals s_1 and s_2 corresponding to adjacent positions x_1 and x_2, formulated by [11]

$$\frac{\mathrm{FT}\left[\mathrm{s}_2(t)\right]}{\mathrm{FT}\left[\mathrm{s}_1(t)\right]} = \left|\frac{\mathrm{s}_2(f)}{\mathrm{s}_1(f)}\right| \mathrm{e}^{\mathrm{i}k(x_2 - x_1)} = \left|\frac{\mathrm{s}_2(f)}{\mathrm{s}_1(f)}\right| \mathrm{e}^{\mathrm{i}\Delta\varphi}. \tag{9}$$

The group velocity is the velocity with which the envelope of wave travels through space. The wave envelope is a group of waves that travel together with similar but distinct frequencies and varying wave velocities. The group velocity can be used for mode identification and damage location in structural health monitoring or non-destructive testing. As in dispersive medium, the group velocity can be experimentally measured by placing two receiving transducers at positions x_1 and x_2 with a distance Δx and extracting time delay of incident wave between two receiving transducers. The group velocity c_{g} can be calculated as:

$$c_{\mathrm{g}} = \frac{\Delta x}{\Delta t}, \tag{10}$$

where Δt is the time delay between two received signals. The wave envelope can be obtained by applying Hilbert transform. Time delay between two received signals can be obtained by solving Cross-correlation function of two envelopes and extracting the maximum. The Cross-correlation function is formulated as:

$$R_{s_1 s_2}(\tau) = \int_{-\infty}^{\infty} s_1(t) s_2(t+\tau) \mathrm{d}t, \tag{11}$$

where τ is the time delay when $R_{s_1 s_2}$ reaches its maximum.

3 3D FE simulations of interaction of A_0 mode Lamb waves with delamination

The 3D FE simulations are carried out using Matlab scripts to create input file for ABAQUS. The specimens are 16-layer CF/EP laminated composite beams. Stacking sequence and material properties are described in sect. 2.1. The dimensions of the composite beams are 500 mm (length) × 30 mm (width) × 2.24 mm (thickness), as shown in Figure 4. In FE simulations, the layers of the beams are individually modeled and their properties are assigned. For the sake of simplicity, no damping is considered in the FE model. The mode of excitation is A_0 with a center frequency of 200 kHz based on the theoretical consideration in sect. 2. Phase velocity and wavelength of this certain mode are 1389 m/s, 6.95 mm respectively. The element chosen is linear, 8-node, 3-dimensional brick type element (C3D8R). As the beam is meshed to 16 layers in thickness, the element size in thickness (z direction) is 0.14 mm. The element size in length (x direction) and in width (y direction) are both 0.5 mm. An incremental time step of 0.02 μs is chosen in the FE models for this investigation. The size of the element and incremental time step meet the convergence conditions described in sect. 2.

FE mesh of composite beam is schematically illustrated in Figure 5 in 2D view. In case of composite beam sample with delamination damage, the delamination in the specimen is modeled by node separation. As shown in Figure 5(b), the nodes across the interface of delamination share the same coordinate values while they have different node numbers, attaching to adjacent elements. No contact mechanism between two surfaces of delamination is considered.

The mode shape of A_0 mode at 200 kHz, as described in sect. 2, reveals that the in-plane displacement is zero at the middle of beam in thickness while out-of-plane displacement is the main component in that position. A concentrated force of the selected waveform with a 5-cycle 200 kHz sinusoidal toneburst modulated by a Hanning window is applied at nodes on the middle of left end of composite beam, as schematically illustrated in Figure 4. In this way, a pure A_0 mode can be excited.

3.1 A_0 mode Lamb wave propagation in defect-free composite beam

Wave propagation in a defect-free composite beam is studied to verify the validity of the FE model. The time history of out-of-plane displacement (displacement in the z direction) at point A and point B are plotted in Figure 6(a). The frequency spectra of the two received signals are shown in Figure 6(b).

It is observed that the bandwidth at −6 dB of the received signals is 76.3 kHz and the peak frequency is about 200 kHz. Using the method described in sect. 2.4, phase velocities of these frequencies are calculated, as plotted in Figure 7. FE simulation results show good agreement with theoretical dispersion curve of A_0 mode, demonstrating the validity and effectiveness of the proposed FE model.

3.2 The interaction of A_0 mode Lamb waves with delamination

To reveal mechanisms of the interaction between A_0 mode Lamb waves and delamination, we investigate a composite beam specimen with through-width delamination, as schematically illustrated in Figure 4, in this section. The delamination has a length of 20 mm and is introduced between the fourth and the fifth layers through node separation.

The snapshots of the displacement fields at different time instants are presented in Figure 8. The snapshot at 150 μs shows the incident A_0 mode Lamb waves propagate near the left end of delamination. Incident wave separates into two parts with different velocities propagating in sub-laminates, as shown in the snapshot at 168 μs. The snapshot at 176 μs shows that little reflection and mode conversion occurs at the left end of delamination. According to the snapshot at 186 μs, large reflection happens at the right end of delamination and considerable wave energy transmits across delamination. The snapshot at 200 μs shows that the waves reflected from the right end of delamination are transmitted across the left end of delamination and parts of the waves

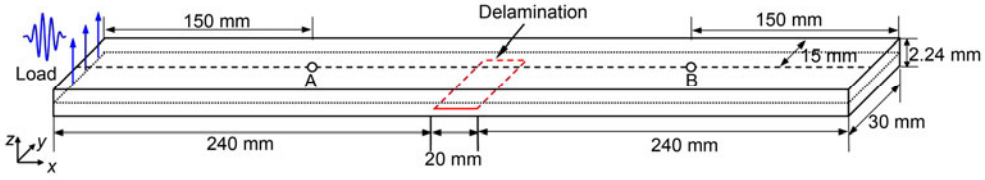

Figure 4 (Color online) Composite beam model specifications used for FE simulation.

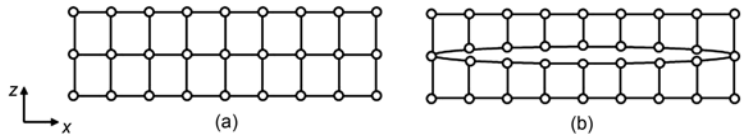

Figure 5 FE mesh of the composite beam sample: (a) no delamination, (b) with delamination.

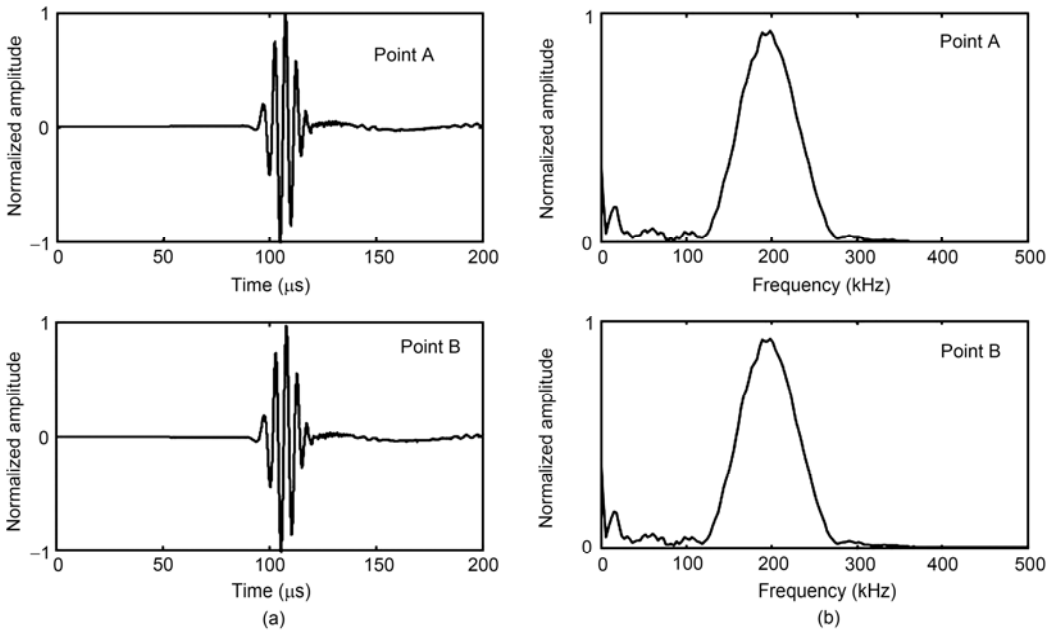

Figure 6 Responses at point A and point B: (a) time history of out-of-plane displacement, (b) frequency spectra.

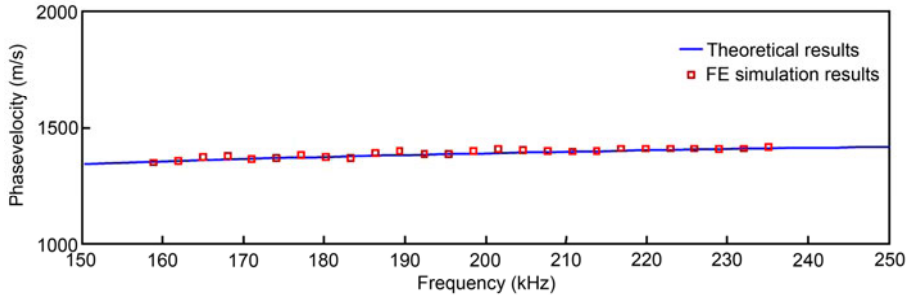

Figure 7 (Color online) Phase velocity dispersion curves of A_0 mode.

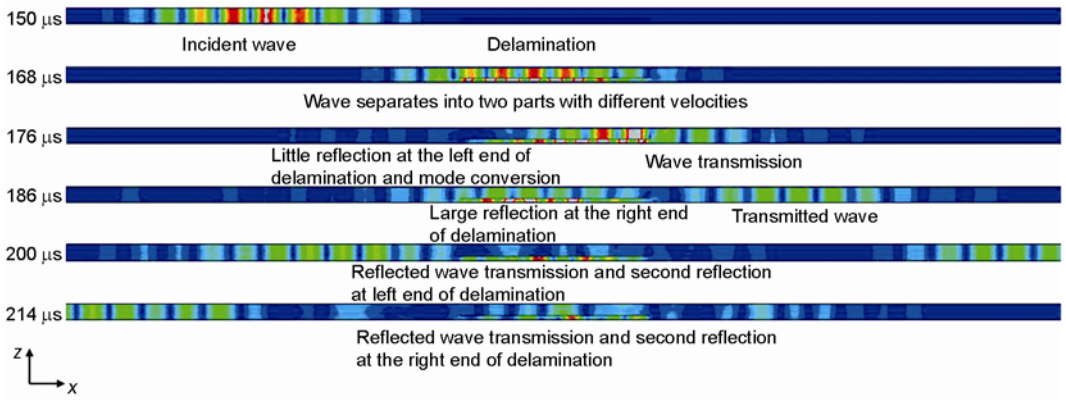

Figure 8 Snapshots of displacement fields at different time instants.

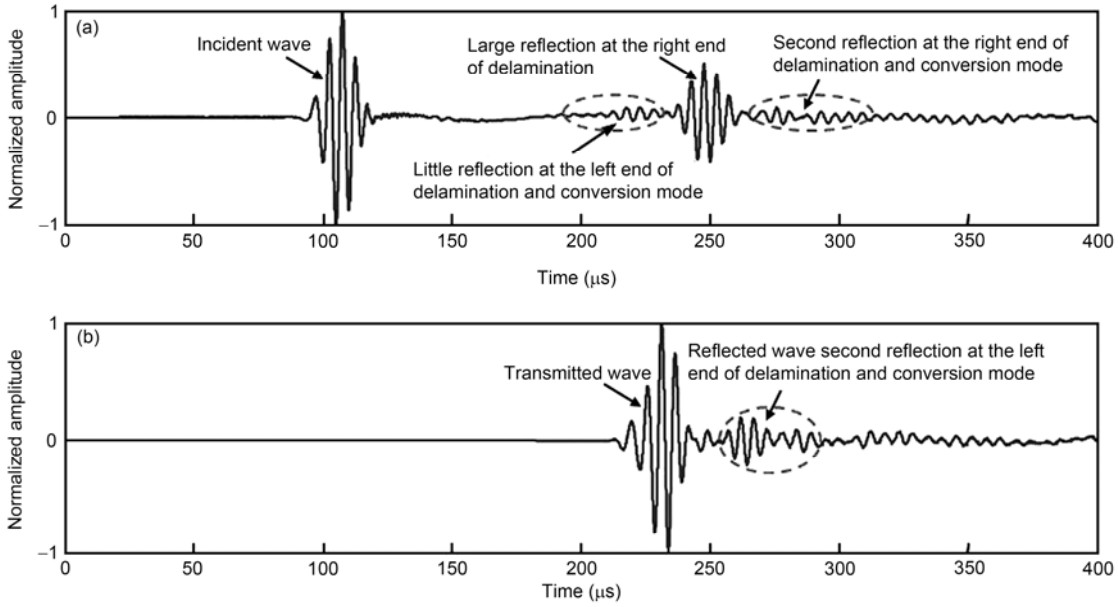

Figure 9 Time history of out-of-plane displacement of Lamb waves at two locations. (a) Time history of out-of-plane displacement at point A. (b) Time history of out-of-plane displacement at point C.

are further reflected at the left end of delamination. The snapshot at 214 μs reveals that waves reflected from the left end of delamination are transmitted across the left end of delamination and parts of the waves are again reflected at the right end of delamination.

Time history of out-of-plane displacement at two locations (point A and point C) are plotted in Figure 9. The transducer at point A can capture the incident wave, reflected waves from the left end of delamination and multiple reflected waves from the right end of delamination. The transducer at point C can capture transmitted wave and reflected waves from the left end of delamination. Transmitted waveform distortion is also observed after comparison with the incident wave.

The FE simulation results reveal that little reflection occurs when the waves propagate from the main laminate to sub-laminates and large reflection will happen when the waves propagate from the sub-laminates to the main laminate. Transmitted waveform distortion can detect the presence of delamination qualitatively. The location and size of delamination can be evaluated quantitatively by extracting arrival time of the waves reflected from both ends of delamination.

4 Experimental investigation

The experimental setup consists of a high power signal generator, a high dB preamplifier, a personal computer (PC), an oscilloscope and a scanning mechanism. The schematic diagram of experimental setup is shown in Figure 10, where the Ritec-RAM5000 ultrasonic measurement system is used to generate high power toneburst voltages for excitation of the air-coupled transmitting transducer and receive signal of the air-coupled receiving transducer with its preamplifier. A pair of transducer fixtures is used to hold and orient the air-coupled ultrasonic transducers at a special angle for excitation and collection of Lamb waves. The air-coupled ultrasonic transducers are gas matrix piezoelectric composite transducers produced by the Ultran Group (Model: NCG200-D13). The center frequency of these transducers is 200 kHz. The composite beam specimens are 16-layer CF/EP composite laminate, as described in sect. 2.1. Lamb waves are excited and propagate along 0° direction of composite laminate. The excitation signal is also a 5-cycle 200 kHz sinusoidal toneburst modulated by a Hanning window.

4.1 Excitation of a pure Lamb wave mode

The influence of incident angle on the excited mode is firstly investigated. A defect-free specimen with the dimensions of 800 mm (length)×30 mm (width)×2.24 mm (thickness), as shown in Figure 11, is investigated. The transducer arrangement is illustrated in Figure 11. As shown in Figure 11, the transmitting transducer is at 225 mm from the left end of the specimen. The receiving transducer is positioned at 150 mm and 200 mm respectively, with respect to the transmitting transducer. The receiving angle θ_R is kept equal to incident angle θ_Γ, so that the receiving transducer is also sensitive to and able to capture the same Lamb wave mode excited by the transmitting transducer.

Angle-scan, making the incident angle θ_Γ varying from

0° to 30° with an angle increment of 2°, is performed with the air-coupled ultrasonic transducer pair. Post signal processing is executed to obtain Angle-scan images, as shown in Figure 12, whose *x*-axis is time domain, *y*-axis is incident angle and *z*-axis is Hilbert envelope amplitude of the received signals. Wavelet transform is applied to denoise the received signals. Hilbert transform is performed to get the envelopes of the received signals. It is observed that there is a small wave packet between 100 and 150 μs when the incident angle is around 4°, and the small wave packet tends to disappear with the increase of the incident angle. A prominent wave packet between 150 μs and 200 μs emerges when the incident angle is around 15°, and reaches its maximum amplitude when the incident angle is 14°. Received signals at these two special angles are plotted in Figure 13.

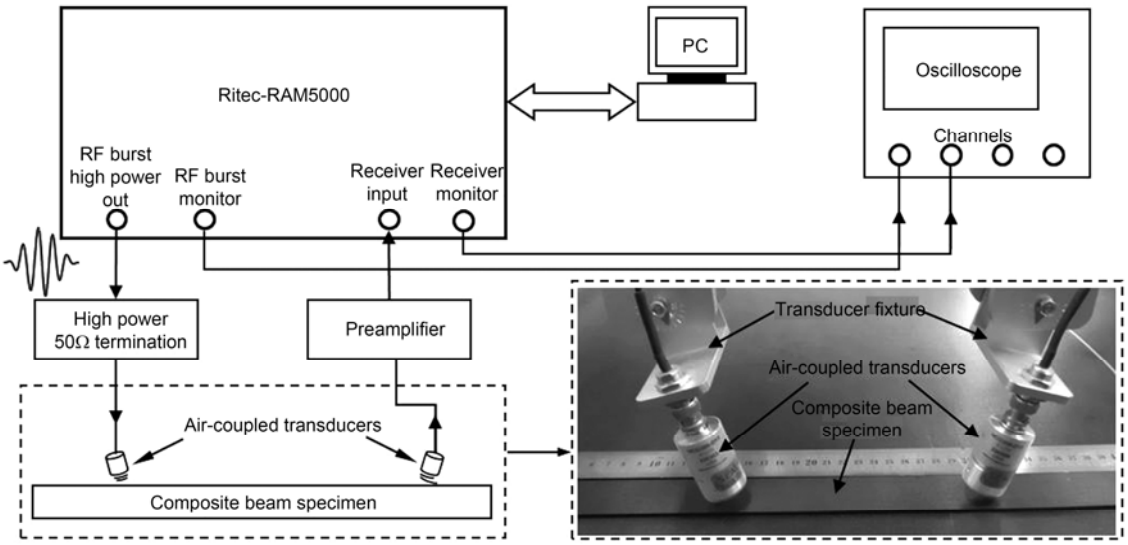

Figure 10 Schematic diagram of the experimental setup.

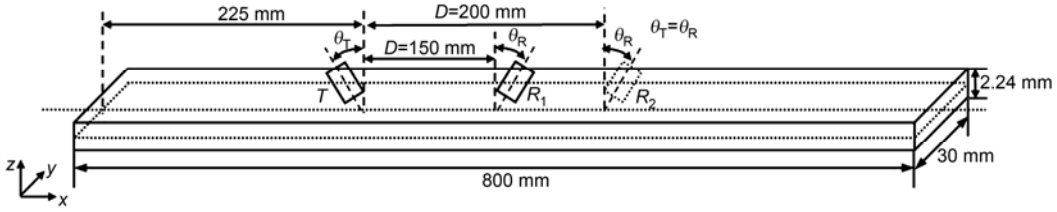

Figure 11 Transducer arrangement for the excitation and reception of a pure Lamb wave mode.

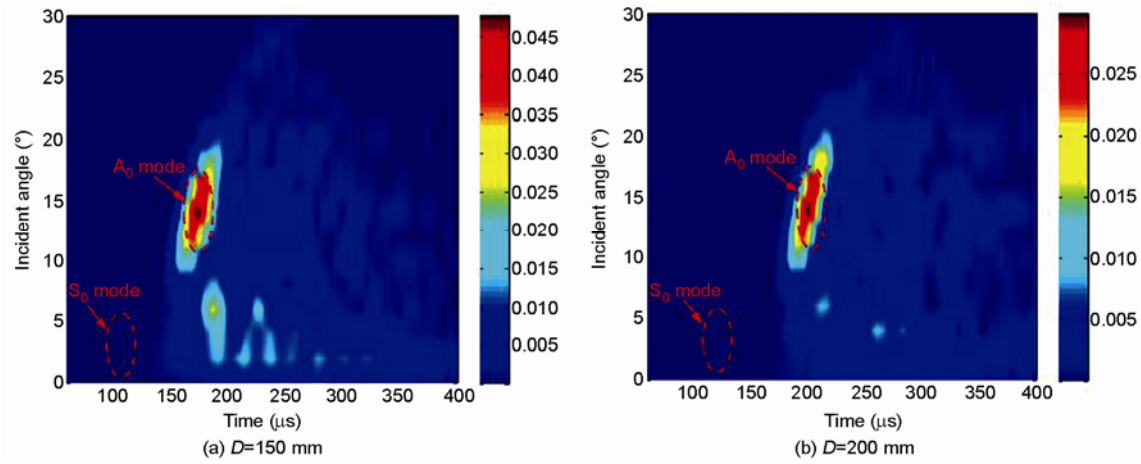

Figure 12 Angle-scan images for the transducers pair with a distance of 150 mm and 200 mm.

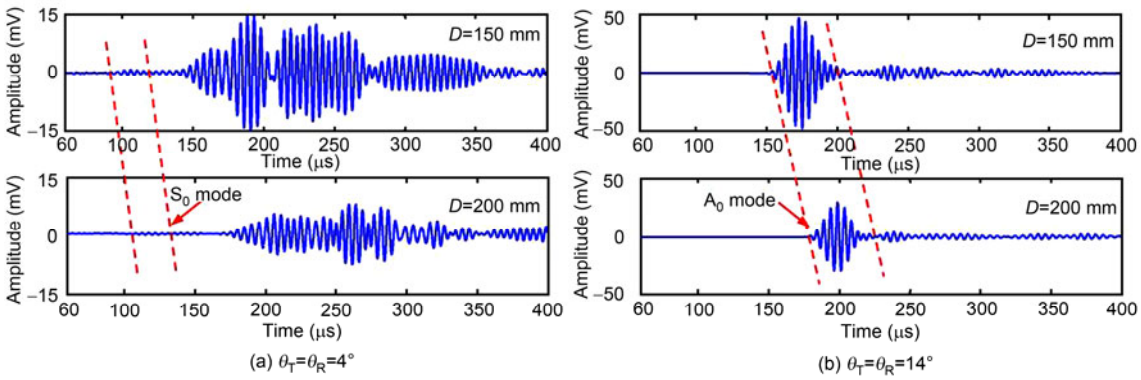

Figure 13 (Color online) Received signals under the incident angles of 4° and 14°.

The group velocity of a particular wave packet is often used for mode identification in practice, as the group velocities of different Lamb wave modes are usually not identical. Using the method described in sect. 2.4, the group velocity of the first small wave packet with the incident angle of 4° and the group velocity of the first large wave packet with the incident angle of 14° are calculated. It is demonstrated that S_0 mode is excited when the incident angle is 4°and A_0 mode is excited when the incident angle is 14° based on the group velocity dispersion curves. The group velocity of A_0 mode is calculated as 1941 m/s. It is also observed that air-coupled ultrasonic transducers are sensitive to anti-symmetric Lamb wave mode because of its large out-of-plane surface displacement. A pure A_0 mode can be excited when the incident angle is 14°. The results and conclusions of this work are in good accordance with previous finite element calculations described in sect. 2.

4.2 Delamination inspection in the composite beam

The interaction of A_0 mode Lamb waves with delamination is investigated experimentally with air-coupled ultrasonic transducers in this section. The dimensions of composite beam specimen are 800 mm (length) × 30 mm (width) ×2.24 mm (thickness), as shown in Figure 14. Through-width delamination damage is introduced by inserting Teflon film (0.05 mm in thickness) between selected layers during the lay-up procedure. The delamination damage is inserted between the fourth and fifth layers and has a length of 20 mm in this study. Along the direction of wave propagation, the receiving transducer is placed in front of and behind the delamination to capture the transmitted and reflected waves introduced by the delamination, respectively. As illustrated in Figure 14, θ_T, θ_{R_1} and θ_{R_2} are all set to be 14° for the excitation and reception of pure A_0 mode signals.

In case of transmitted wave detection, the receiving transducer R_1 is placed behind the delamination with a distance L_{d_1}, with respect to the right end of delamination. The receiving transducer is oriented to be sensitive to the wave propagating in the same direction as incident wave. The length of L_{d_1} is increased from 20 mm to 60 mm with a step of 10 mm. Received signals are plotted in Figure 15. The first wave packet is the waves transmitted across the delamination. Reflected waves further reflected at the left end of the delamination are observed when L_{d_1} is 20 mm and 30 mm.

In case of reflected wave detection, the receiving transducer is placed in front of the delamination with a distance L_{d_2}, with respect to the left end of delamination. The length of L_{d_2} is increased from 20 mm to 60 mm with a step of 10 mm. The received signals are shown in Figure 16. Wave

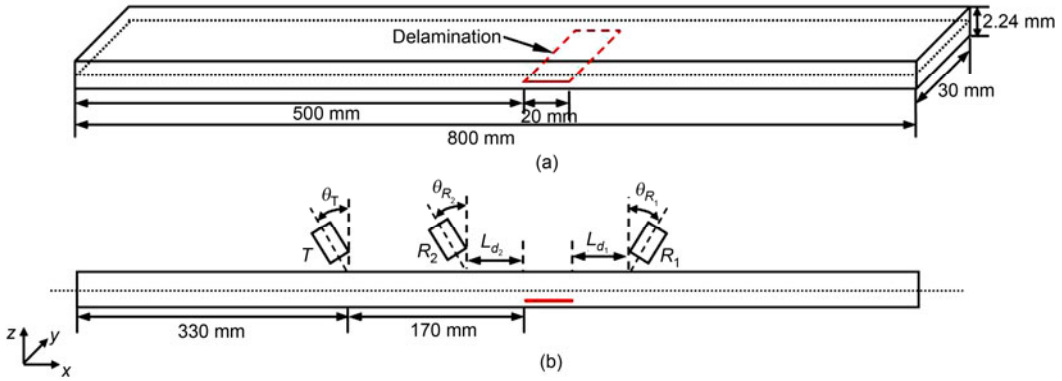

Figure 14 (Color online) Beam specimen and transducer arrangement for the study on wave interaction with the delamination. (a) Beam specimen with delamination; (b) Transducer arrangement.

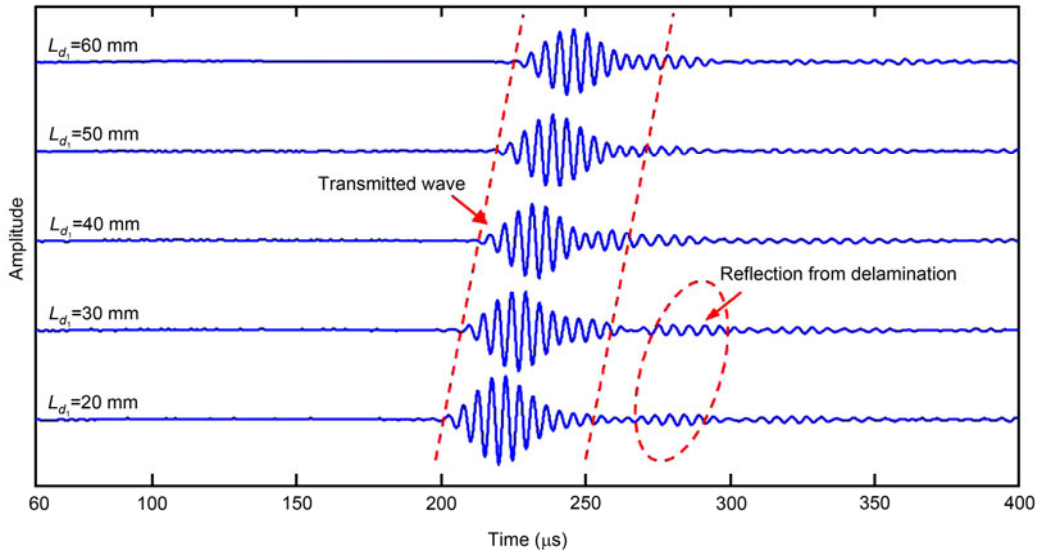

Figure 15 (Color online) Received signals of the transducer placed behind the delamination.

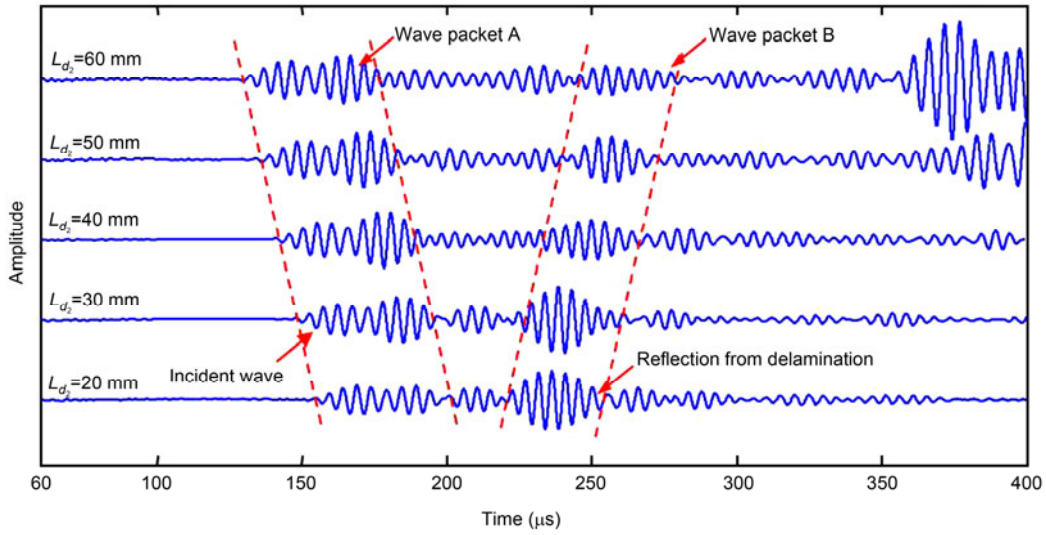

Figure 16 (Color online) Received signals of the transducer placed in front of the delamination.

packet A, as labeled in Figure 16, advances in the time domain as L_{d_2} increases. It is demonstrated that wave packet A is the leaky incident wave. However, the amplitude of wave packet A is small because the orientation of the receiving transducer makes it more sensitive to waves propagating in contrast to incident waves. Wave packet B delays in the time domain as L_{d_2} increases. The amplitude of wave packet B is even larger than that of incident wave. We can conclude that wave packet B is reflected wave. Assume that the wave packet B is reflected from the left end of the delamination as case I and from the right end of the delamination as case II. The experimental wave propagation path difference between wave packets A and B are obtained through calculating the time-of-flight (TOF) difference between wave packets A and B as the group velocity is calculated in sect. 4.1. The experimental and theoretical wave propagation path differences are presented in Table 2, respectively. The results in Table 2 confirm that wave packet B is reflected from the right end of the delamination. The waves between wave packets A and B are mode conversion wave and wave reflected from the left end of the delamination. It is demonstrated that little reflection occurs when waves propagate from the main laminate to the sub-laminates (delamination area) meanwhile large reflection will happen when waves propagate from the sub-laminates to the main laminate.

5 Conclusion

The interaction of A_0 mode Lamb waves with delamination in laminated composite beams is investigated through 3D

Table 2 Wave propagation path difference

L_{d_2} (mm)	Experimental wave propagation path difference (mm)	Wave path propagation difference of case I (mm)	Wave path propagation difference of case II (mm)
20	85.63	40	80
30	108.46	60	100
40	137.34	80	120
50	162.50	100	140
60	173.06	120	160

FE simulation and experiments. It is demonstrated that little reflection occurs when waves propagate from the main laminate to the sub-laminates and large reflection will happen when waves propagate from the sub-laminates to the main laminate. Waveform distortion happens when the incident wave propagates across the delamination area. For the purpose of quantitative detection of delamination, post signal processing like Hilbert transform and Cross-correlation should be performed to the extract arrival time of waves reflected from both ends of the delamination. The location and size of delamination can be evaluated quantitatively by capturing waves reflected from both ends of the delamination.

As acoustic impedance mismatch between air and composite materials is not so serious, non-contact ultrasonic testing of composite materials with air-coupled ultrasonic transducers is attractive in practice. The finite element analysis results show that a pure Lamb wave mode can be excited and detected by the appropriate arrangement of transducers. Angle-scan images obtained with air-coupled ultrasonic transducers demonstrate that pure A_0 mode Lamb waves can be excited and detected efficiently. Results also reveal that transducer orientation makes it showing different sensitivity to waves propagating in different directions.

This work was supported by the National Natural Science Foundation of China (Grant Nos. 11272021 and 50975006), Beijing Natural Science Foundation (Grant No. 1122007), the Importation and Development of High-Caliber Talents Project of Beijing Municipal Institutions (No. CIT&TCD201304048) and Beijing Nova Program (Grant No. 2008A015)

1 Islam A S, Craig K C. Damage detection in composite structures using piezoelectric materials. Smart Mater Struct, 1994, 3: 318–328
2 Su Z, Ye L, Lu Y. Guided Lamb waves for identification of damage in composite structures: a review. J Sound Vib, 2006, 295: 753–780
3 Guo N, Cawley P. The interaction of Lamb waves with delaminations in composite laminates. J Acoust Soc Am, 1993, 94: 2240–2246
4 Ramadas C, Balasubramaniam K, Joshi M, et al. Interaction of the primary anti-symmetric Lamb mode (A_0) with symmetric delaminations: Numerical and experimental studies. Smart Mater Struct, 2009, 18: 085011
5 Peng H K, Ye L, Meng G, et al. Concise analysis of wave propagation using the spectral element method and identification of delamination in CF/EP composite beams. Smart Mater Struct, 2010, 19: 085018
6 Schindel D W, Hutchins D A. Through-thickness characterization of solids by wideband air-coupled ultrasound. Ultrasonics, 1995, 33: 11–17
7 Peters J, Kommareddy V, Liu Z, et al. Non-contact inspection of composites using air-coupled ultrasound. Thompson D O, Chimenti D E, eds. In: Review of Progress in Quantitative Nondestructive Evaluation, Washington, USA, 2003. 973–980
8 Luukkala M, Meriläinen P. Metal plate testing using airborne ultrasound. Ultrasonics, 1973, 11: 218–221
9 Briks A S, Green R E. Nondestructive Testing Handbook: Ultrasonic Testing. Ohio: American Society for Nondestructive Testing, 1991. 837–839
10 Castaings M, Cawley P, Farlow R, et al. Single sided inspection of composite materials using air coupled ultrasound. J Nondestr Eval, 1998, 17: 37–45
11 Castaings M, Hosten B. Lamb and SH waves generated and detected by air-coupled ultrasonic transducers in composite material plates. NDT&E Int, 2001, 34: 249–258
12 Kazys R, Demcenko A, Zukauskas E, et al. Air-coupled ultrasonic investigation of multi-layered composite materials. Ultrasonics, 2006, 44: e819–e822
13 Bhardwaj M. Phenomenally high transduction air/gas transducers for practical non-contact ultrasonic applications. Thompson DO, Chimenti DE, eds. In: Review of Progress in Quantitative Nondestructive Evaluation, Chicago, USA, 2009. 920–927
14 Yan F, Hauck E, Pera T M, et al. Ultrasonic guided wave imaging of a composite plate with air-coupled transducers. Thompson DO, Chimenti DE, eds. In: Review of Progress in Quantitative Nondestructive Evaluation, Oregon, USA, 2007. 1007–1012
15 Takahashi S, Ohigashi H. Ultrasonic imaging using air-coupled P(VDF/TrFE) transducers at 2 MHz. Ultrasonics, 2009, 45: 495–498
16 Raišutis R, Kažys R, Žukauskas E, et al. Ultrasonic air-coupled testing of square-shape CFRP composite rods by means of guided waves. NDT&E Int, 2011,44: 645–654
17 Schmidt F, Rheinfurth M, Protz R, et al. Monitoring of multiaxial fatigue damage evolution in impacted composite tubes using non-destructive evaluation. Compos Part A-Appl Sci Manuf. 2012, 43: 537–546
18 Rose J L. Ultrasonic Waves in Solid Media. Cambridge: Cambridge University Press, 1999. 10–15
19 Lowe M J S. Matrix techniques for modelling ultrasonic waves in multilayered media. IEEE Trans Ultrason Ferroelectr Freq Control, 1995,42: 525–542
20 Viktorov I A. Rayleigh and Lamb waves. New York: Plenum Press, 1967
21 Castaings M, Cawley P. The generation, propagation and detection of Lamb waves in plates using air-coupled ultrasonic transducers. J Acoust Soc Am, 1996, 100: 3070–3077
22 Bathe K J. Finite Element Procedures in Engineering Analysis. New Jersey: Prentice-Hall, 1982. 30–50
23 Moser F, Jacobs L J, Qu J M. Modeling elastic wave propagation in waveguides with the finite element method. NDT&E Int, 1999, 32: 225–234
24 Alleyne D, Cawley P. A two-dimensional Fourier transform method for the measurement propagating multimode signals. J Acoust Soc Am, 1991, 89: 1159–1168